Experimental study of humidity distribution inside electronic enclosure and effect of internal heating

Conseil, Helene; Jellesen, Morten Stendahl; Ambat, Rajan

Published in:
Proceedings of the European Corrosion Congress : EUROCORR 2015

Publication date:
2016

Document Version
Peer reviewed version

Experimental study of humidity distribution inside electronic enclosure and effect of internal heating

Hélène Conseil, Morten S. Jellesen and Rajan Ambat
Materials and Surface Engineering, Department of Mechanical Engineering,
Technical University of Denmark, Hélène Conseil
Building 425, Kongens Lyngby, Denmark, helco@mek.dtu.dk

Summary

Corrosion reliability of electronic products is a key factor for electronics industry, and today there is a large demand for performance reliability in a wide range of temperature and humidity during day and night time periods. Corrosion failures are still a challenge due to the combined effects of temperature, humidity and corrosion accelerating species in the atmosphere. Moreover the surface region of printed circuit board assemblies is often contaminated by various aggressive chemical species.
This study describes the overall effect of the exposure to severe climate conditions and internal heat cycles on the humidity and temperature profile inside typical electronic enclosures. Defined parameters include external temperature and humidity conditions, temperature and time of the internal heat cycle, thermal mass, and ports/openings size. The effect of the internal humidity on electronic reliability has been tested by measuring the leakage current on inter-digitated test comb patterns which are pre-contaminated with sodium chloride and placed inside the enclosure.
Results showed that exposure to cycling temperature leads to a significant change of internal water vapour concentration, where the maximum value was function of the opening size and the presence of thermal mass inside the enclosure. A pumping effect was observed and the increase of the level of absolute humidity at each cycle lead to condensation, corresponding to a sudden increase in leakage current of the test patterns pre-contaminated with sodium chloride. The changes of internal temperature and humidity can lead to water condensation and evaporation cycles which can cause electrical failures.

Key words: Humidity, temperature, electronic materials, enclosures, internal climate, electronic reliability.

I. Introduction

Electronic products are exposed to various kinds of climatic conditions; therefore the protection of these devices is a critical factor in design of systems. Moist as well as condensing environments during application of these systems can significantly alter the enclosed electronic device's performance. The observed consequences of this phenomenon are reduced life span of the products and heavy economic loss due to failures.
The protection of an electronic product against a harsh environment highly depends on the design of enclosure. The enclosure body needs to be designed to provide holes/openings for cooling, input-output ports for electrical connections, hinges, screw locations, and so forth [1]. An electronic enclosure is hence seldom perfectly sealed, and the moisture

ingress is dependent of the moisture diffusion through the walls, through the surrounding sealants, and also through the eventual leaks [2]. Thermal mass are widely used in electronics. In common use, it is a metal object brought into contact with an electronic component's hot surface. The high thermal conductivity of the metal combined with its large surface area results in the rapid transfer of thermal energy to the surrounding, cooler, air. The temperature is reduced through increased heat dissipation.

Corrosion occurs due to the interaction of heat, moisture and stress in a material. The presence of ionic residues on the printed circuit board assemblies (PCBA) surface, arising from the soldering process [3] [4] [5] [6] [7], contamination in the materials used during manufacturing, or the species derived from the surrounding environment (gases, aggressive ions, dust etc.) [8] [9] [10] [11] [12] [13], will also reduce the level of humidity at which failures (corrosion and electrochemical metal migration) can occur on the PCBAs.
The tests have been performed to determine the internal climate profile of a polycarbonate enclosure and the electronic corrosion reliability resistance of a PCB placed inside and exposed to a cycling elevated temperature and high humidity environment, under a nominal run state static bias. In this test, the internal heating and outside cycling temperature test are used to simulate alternate power/temperature extremities. The effect of the leak/opening size, the presence and volume of a thermal mass and the concentration of NaCl contamination on the PCB are the three variables that are investigated.
Leakage current (LC) measurement was used for assessing the electrical effect of surface contamination on a PCB, and for determining any metal migration, corrosion, or dielectric breakdown. The level of leakage current is also an indication of the degree of water layer formation on the PCB surface, and reveals the condensing period to which the electronic circuit board is exposed. The PCB was placed at the centre of the enclosure on an aluminium plate (commonly used thermal mass material). The thermal mass is undergoing nearly instantaneous change in temperature and moisture can be accumulated by the pumping effect.

II. Materials and methods

1. Climate investigations

The investigated enclosures were made of polycarbonate and have the dimensions of (280 mm x 190 mm x 130 mm). A through hole of 1 or 3 mm diameter has been drilled on one side of the enclosure in order to simulate a possible leakage opening. Calibrated sensors were placed in the enclosures, to monitor the temperature and relative humidity (RH) (PT1000 and HIH4021, Honeywell), connected to a data logging system (Model 2700 Multimeter, Keithley Instruments). The enclosures are exposed to a constant RH of 98%, and to a cycling temperature of 50 ˚C during one hour and of 10 ˚C during two hour, in a climatic chamber (Espec, Escorp PL-3KPH). A heating element (silicon mat type) was also introduced in the enclosure in order to simulate the heat generated from the components on PCBA during the ‘ON’ time of the electronic device. The heating element was switched on for duration of 45 min, and switched off for duration of 2 h and 15 min in order to have a 15 min delay from the start of heating up at 50 ˚C (cf. the profile in Fig. 1).

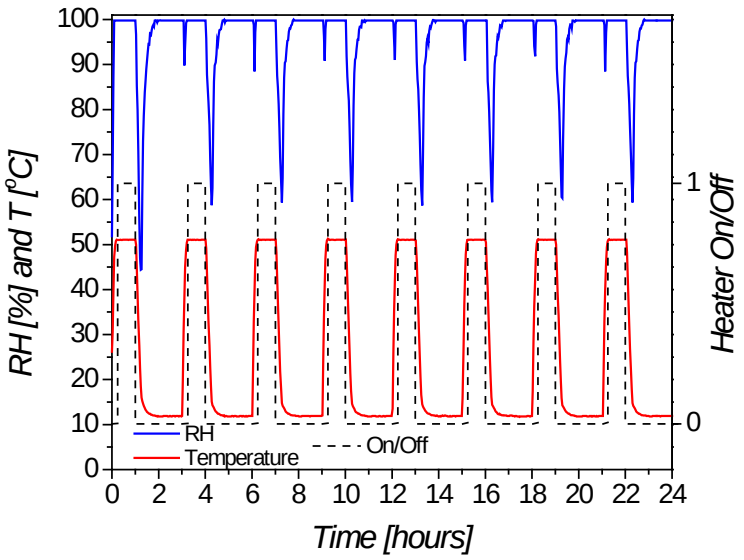

Figure 1: Measured climate profile in the climatic chamber, with internal heating profile

2. Corrosion reliability and water layer formation

Leakage current (LC) measurement was used for assessing the effect on electrical conductivity, of humidity and temperature cycles, and of the contamination of the surface of a PCB. The PCBA level testing was carried out on a board made in accordance to IPC-4101/21 from a FR4 substrate, with dimensions 168 mm × 112.4 mm and a thickness of 1.6 mm (Figure 2). The surface insulation resistance (SIR) comb pattern used for experiments was a lead containing solder and had the dimensions of 13 mm × 25 mm, and a pitch and spacing size of 0.3 mm. The overlapping area was 10.8 mm in height and there were 41 sets of common overlap providing 442.8 mm as the total length of the opposing faces. The ratio of the total length of the opposing faces and the spacing of segments yields the nominal square count, which is 1476 for this SIR. For reference, the standard IPC-B-36 and IPC-B-24 comb patterns have 3538 and 1020 squares. The sensitivity of an SIR pattern increases with increasing number of squares. Detailed description of the test PCBA is to be found elsewhere [14]. A constant potential bias of 5 V DC was applied to the SIR pattern and the LC was measured constantly during the exposure test (Biologic VSP-series potenstiostat system).

Figure 2: SIR PCB picture

The SIR comb patterns were pre-contaminated with 0 (clean), 1.56 µg·cm^{-2} and 15.6 µg·cm^{-2} of NaCl. The details of the experiment set up can be seen in Table 1. The contamination levels investigated are based on IPC standard J-STD-001D “Requirements for soldered electrical and electronic assemblies”, which specifies a maximum surface

concentration of 1.56 µg·cm^{-2} NaCl equivalents to be allowed in assembled electronic components [15].

Table 1: Experiment details of the enclosure hole size, the size of the thermal mass and the level of NaCl contamination

	1 mm diameter hole at the bottom	3 mm diameter hole at the bottom
Empty	No SIR PCB	No SIR PCB
No thermal mass	1.56 µg· cm^{-2} of NaCl	1.56 µg· cm^{-2} of NaCl
Small thermal mass [8 x 5 x 1] cm^3	1.56 µg·cm^{-2} of NaCl	1.56 µg· cm^{-2} of NaCl
Big thermal mass [10 x 8 x 1] cm^3	0 µg·cm^{-2} of NaCl (Clean)	-
	1.56 µg· cm^{-2} of NaCl	1.56 µg· cm^{-2} of NaCl
	15.6 µg· cm^{-2} of NaCl	15.6 µg· cm^{-2} of NaCl

III. Results

1. Effect of hole diameter on internal temperature and humidity profile

The results of the temperature profile (temperature T, and dew point DP) and moisture ingress (relative humidity RH, and absolute humidity AH) into the enclosures with 1 and 3 mm diameter hole, exposed to the cycling conditions is shown in Fig. 3.

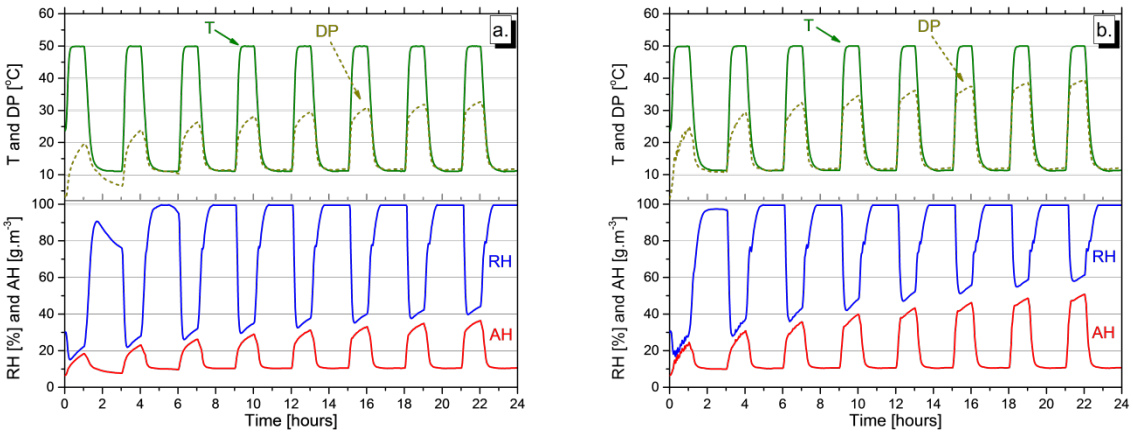

Figure 3: Internal T, DP, RH and AH inside the empty Polycarbonate enclosure exposed to the cycling conditions, with a controlled leakage size of a) 1 mm diameter and b) 3 mm diameter.

The cycling of temperature led to a cycling in humidity inside the polycarbonate enclosures, with an increase of absolute humidity (concentration of water vapour) at every increase of temperature from 10 ˚C to 50 ˚C. The internal temperature followed the external cycling temperature, while the internal humidity showed a different profile. Even if the external RH condition was constant (98% RH), a constant increase of RH at each cycle was observed, when the external temperature raised to 50 ˚C. The saturation of water vapour inside the enclosure was not achieved at that condition (at 50 ˚C, AH = 81 $g.m^{-3}$ according to Mollier diagram). At the last cycle at 50 ˚C, AH = 36 and 51 $g.m^{-3}$ inside the enclosure respectively with 1 and 3 mm diameter hole.

2. Effect of internal heating and thermal mass on internal temperature and humidity profile

The results of the temperature profile and moisture ingress into the enclosure with 1 and 3 mm diameter hole, with an internal heater and a SIR PCB placed on a thermal mass of [8 x 5 x 1] and [10 x 8 x 1] cm^3, exposed to the cycling conditions is shown in Fig. 4.

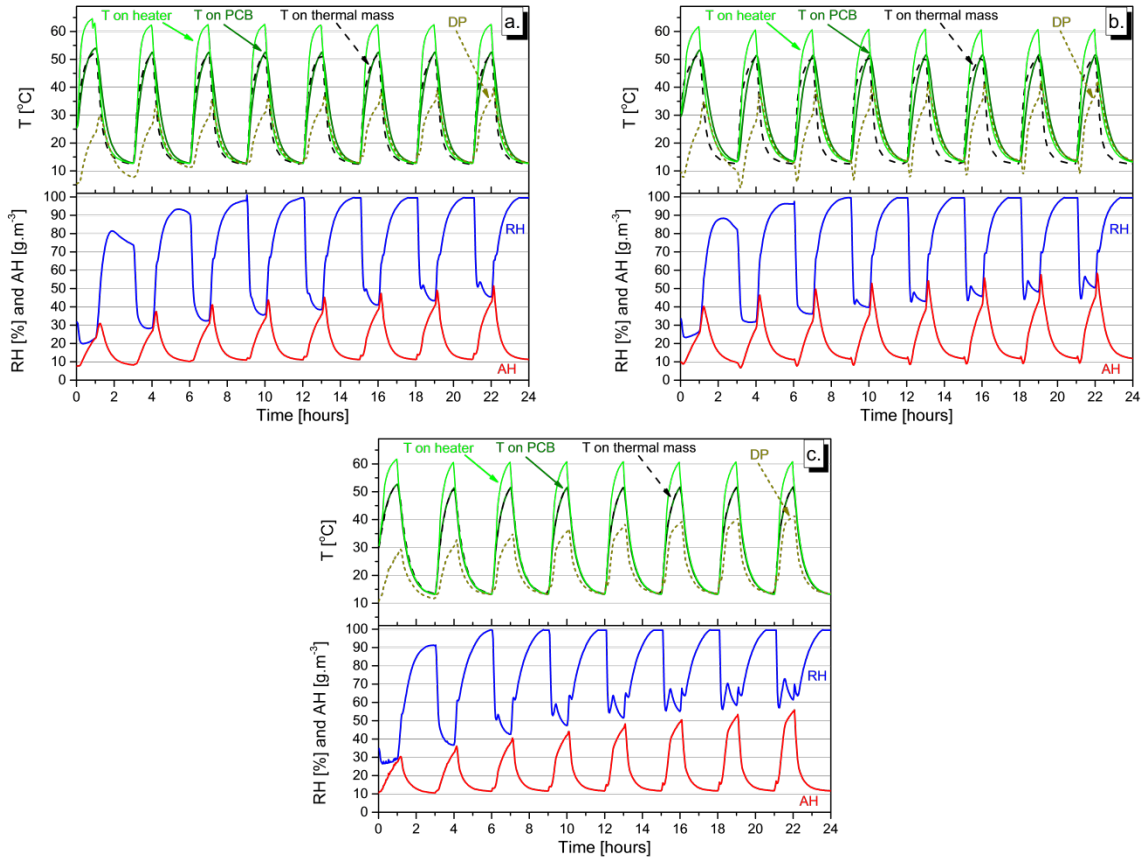

Figure 4: Internal climate in Polycarbonate enclosures exposed to the cycling conditions, with an internal heater and an SIR PCB, with a controlled leak size of 1 mm diameter and a) a thermal mass of [8 x 5 x 1] cm^3, b) a thermal mass of [10 x 8 x 1] cm^3, and c) with a controlled leak size of 3 mm diameter and a thermal mass of [10 x 8 x 1] cm^3

The humidity profiles show that the humidity level (RH and AH) increased at each cycles until a constant internal cycling profile was observed. At the last cycle, the AH ranges inside the enclosures with 1 mm diameter hole and a thermal mass of [8 x 5 x 1] and [10 x 8 x 1] cm^3 were between [12-52] $g \cdot m^{-3}$ and [12-57] $g \cdot m^{-3}$ respectively, while it was between [12-56] $g \cdot m^{-3}$ for the enclosure with 3 mm diameter hole and a thermal mass of [10 x 8 x 1] cm^3. Overall the level of AH has increased in comparison to the level of humidity inside the enclosure without thermal mass (see Fig. **3**). The larger thermal mass has increased the humidity level inside the enclosures (Fig.4.a and Fig.a and b), while the profile change of humidity was broader inside the enclosure with the bigger leak size (Fig.4.c).

The temperatures on the surface of the SIR PCB and on the thermal mass are shown in Fig. 5. The temperature of the thermal mass was approx. 2-3 °C warmer than the surrounding air temperature in the chamber. It can be seen that in the case of the enclosure with an opening of 1 mm diameter, the cooling temperature on the PCB surface has a delay compared to the thermal mass temperature, while their temperatures are similar when placed inside the box with 3 mm diameter. The increase of airflow over the thermal mass has promoted the cooling of the PCB laminate.

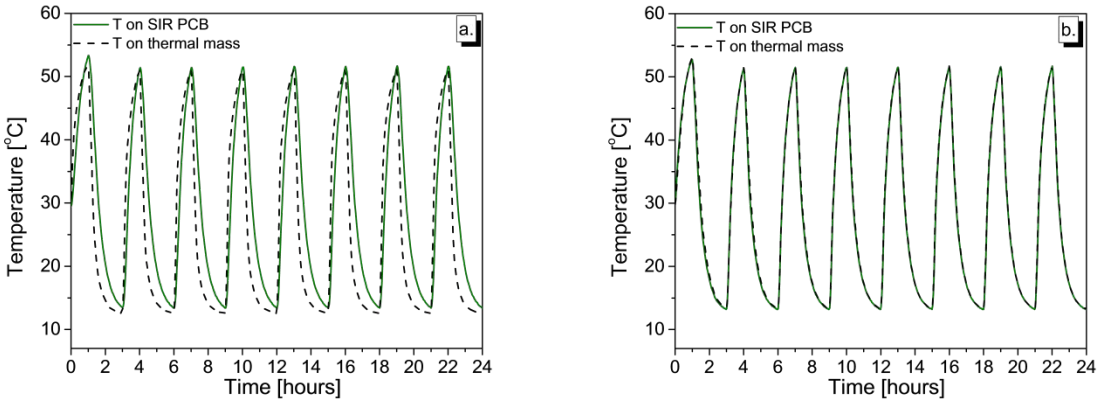

Figure 5: Temperature on the SIR PCB and on the thermal mass [10 x 8 x 1] cm^3, inside the Polycarbonate enclosure exposed to the cycling conditions and with a controlled leak size of a) 1 mm diameter and b) 3 mm diameter

3. Effect of leak size, thermal mass and level of contamination on leakage current

The correlation of leakage current, and leak size, size of thermal mass and level of contamination as a function of cycling time is presented in Fig. 6. The SIR patterns were pre-contaminated with 0, 1.56 and 15.6 $\mu g \cdot cm^{-2}$ of NaCl, and placed at the centre of the enclosure with 1 and 3 mm diameter hole, on a thermal mass of [8 x 5 x 1] cm^3 and of [10 x 8 x 1] cm^3.

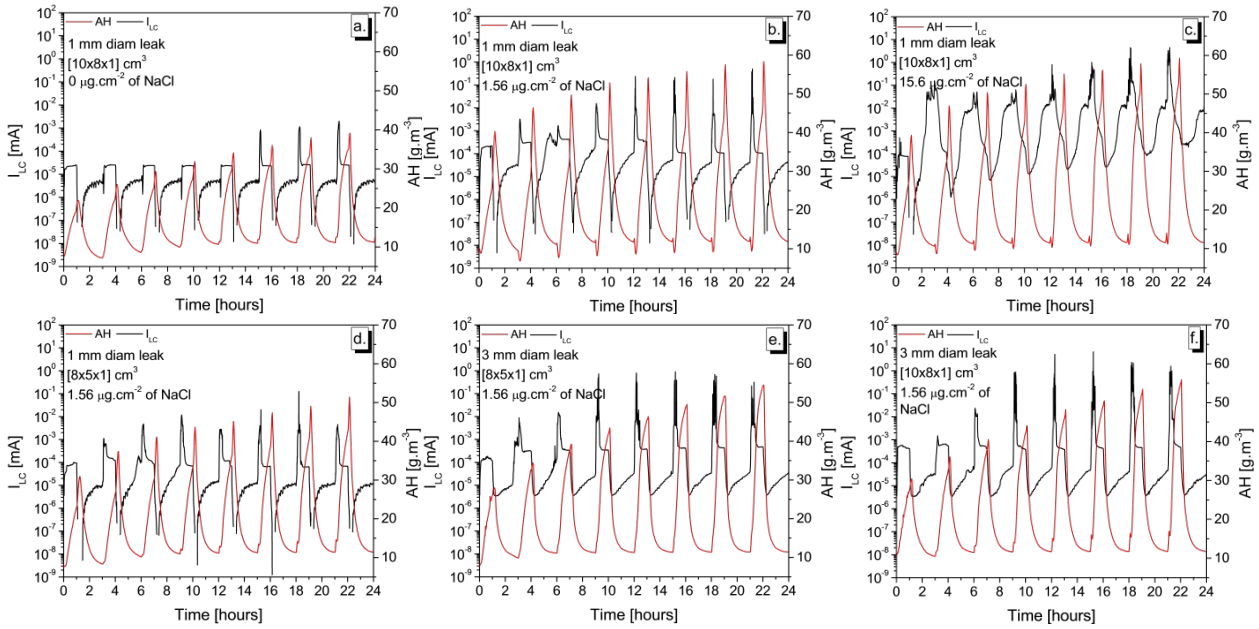

Figure 6: Absolute humidity on PCB´s surface and corresponding leakage current profile on SIR comb pattern pre-contaminated with NaCl, placed at the centre of the enclosure, and at the centre on a thermal mass in Polycarbonate enclosure with 1 and 3 mm diameter leak hole.

The profile obtained on the non-contaminated sample shown in Fig.6.a indicates that the fast change of temperature from 10 ˚C to 50 ˚C led to a high increase of absolute humidity during each cycle inside the enclosure, leading to higher level of leakage current on the SIR PCB surface. This can be attributed to the build-up of water layer on the surface. At 10 ˚C, a thin non-uniform water layer is formed on the surface, with corresponding slow increase of LC, while the sudden increase of water vapour concentration at the rise to 50 ˚C led to an increase of the water layer thickness, and high LC on the SIR surface.

The introduction of NaCl contamination of 1.56 µg·cm^{-2} (Fig.6.b) on the surface of the PCBA did not lead to an increase of LC under low condensing conditions (when temperature was 10 ˚C). However, when higher condensation occurred (when temperature raised to 50 ˚C), the LC difference between non-contaminated samples and samples contaminated with 1.56 µg·cm^{-2} of NaCl was as much as 2-3 orders of magnitude. The contamination level of 15.6 µg·cm^{-2} has increased the overall level of LC, reaching a value of 4 mA (Fig.6.c).

Figures 6.d and 6.e show the effect of the hole size on the AH and LC profile. Higher levels of AH and consequently higher levels of LC are observed for the enclosure with bigger leak size, while even higher LC levels are reached in the presence of larger thermal mass (Fig.6.f).

An overview of the effects of the leak size, the volume of the thermal mass and the contamination level on the LC are presented in Figure 7.

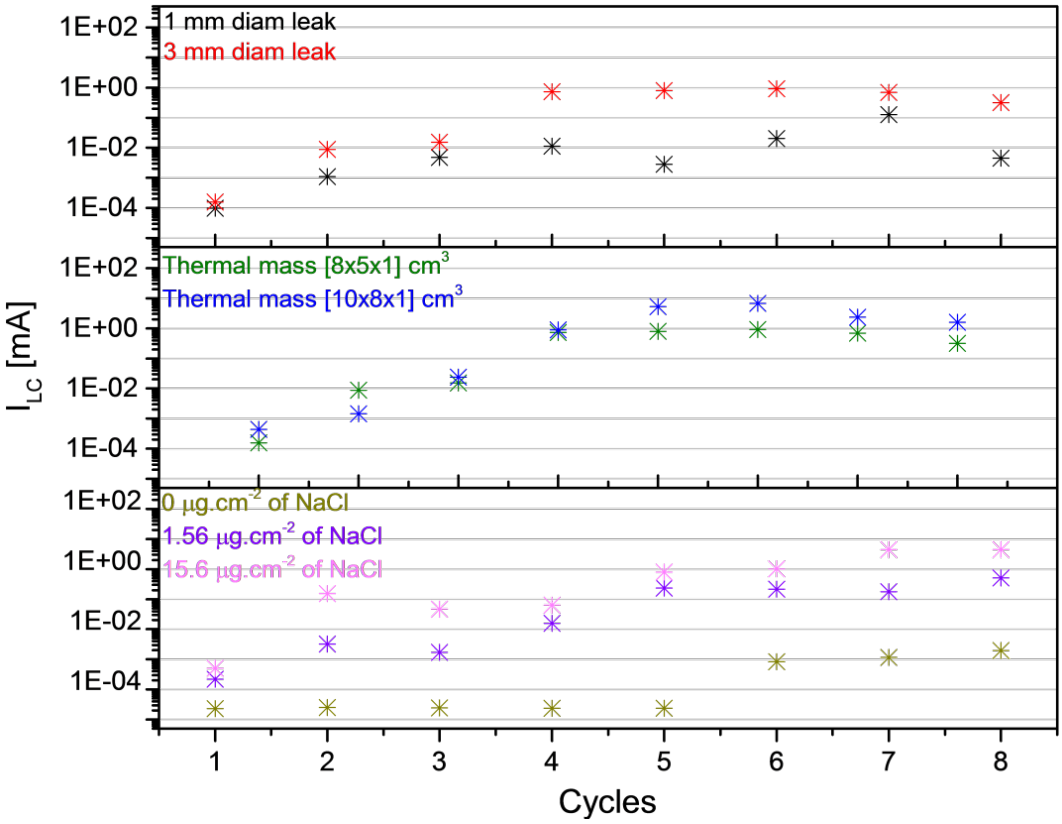

Figure 7: Effect of the leakage size, the volume of thermal mass, and the contamination level on maximal leakage current measured on SIR comb pattern placed inside the Polycarbonate enclosures

The images of the SIR PCB comb patterns after the cycling exposure are shown in Figure 8. Corrosion products appeared on the SIR patterns of the PCB placed on the thermal mass and contaminated with NaCl. The high contamination level of 15.6 µg·cm^{-2} of NaCl has resulted in very high LC and high level of corrosion on the PCB surface.

	Enclosure with a 1 mm diameter hole	Enclosure with a 3 mm diameter hole
0 µg·cm^{-2} of NaCl Thermal mass [10 x 8 x 1] cm^3	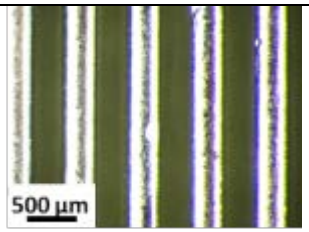	
1.56 µg·cm^{-2} of NaCl No thermal mass	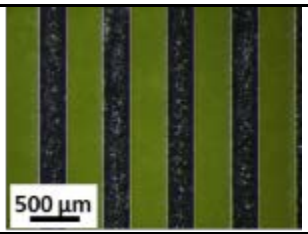	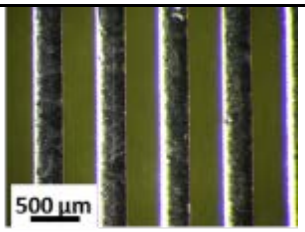

1.56 µg·cm^{-2} of NaCl Thermal mass [8 x 5 x 1] cm^3	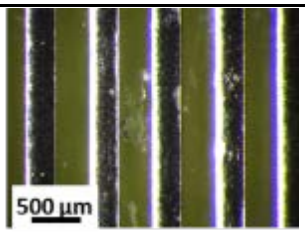	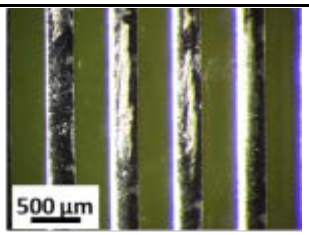
1.56 µg·cm^{-2} of NaCl Thermal mass [10 x 8 x 1] cm^3	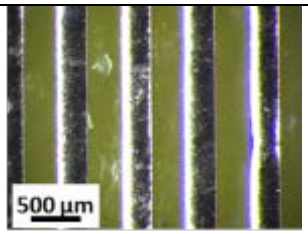	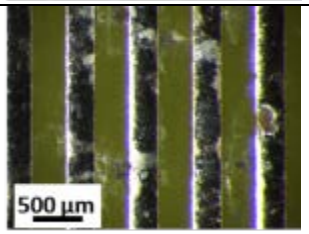
15.6 µg·cm^{-2} of NaCl Thermal mass [10 x 8 x 1] cm^3	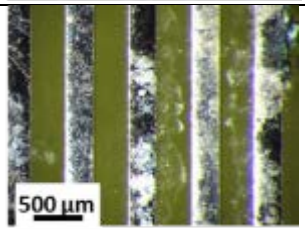	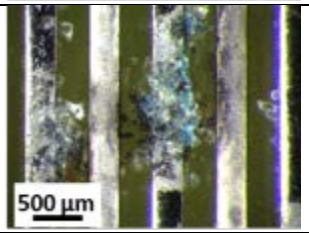

Figure 8: Pictures of the SIR comb pattern after climatic testing at 98%RH and cyclic change of temperature from 10 ˚C to 50 ˚C.

IV. Discussion

The time constant for internal temperature change was low, as shown in Figure 3, while the time constant for humidity change was much slower. Even if the external condition was at 98% RH, the saturation of water vapour inside the enclosure was not attained when the temperature was at 50 ˚C. This is due to the fact that the air has a given capacity to hold water vapour. Warmer air has a greater capacity to hold water vapour than cooler air. (For example, according to Mollier diagram, at 50 ˚C and 98% RH, AH = 81 g.m^{-3}, while at 10 ˚C, AH decreases to 9 g.m^{-3}). Consequently, the total amount of water vapour that the air can hold is primarily a function of its temperature. As air is cooled, its capacity to hold water vapour is diminished. In this experiment, the time of the cycle was shorter than the time constant for water vapour to diffuse through the leak and reach the equilibrium, and at each cycle at 50 ˚C, the AH increased but did not reach its maximal value, while at 10 ˚C the AH was close to its saturation value. When air can no longer hold the water vapour it contains, it is said to be saturated and "condensation" (liquid water) will take place. The overall humidity profile level was higher inside the enclosure with higher leak size (3 mm diameter hole) than with the smaller leak size (1 mm diameter hole).

In thermodynamics, a heat sink is a heat reservoir that can absorb an arbitrary amount of heat without significantly changing temperature. Practical heat sinks for electronic devices must have a temperature higher than the surroundings to transfer heat by convection, radiation, and conduction. The power supplies of electronics are not 100% efficient, so extra heat is produced that may be detrimental to the function of the device. As such, a heat sink is included in the design to disperse heat to improve efficient energy use.

A heat sink's thermal mass can be considered as a capacitor (storing heat instead of charge) and the thermal resistance as an electrical resistance (giving a measure of how fast stored heat can be dissipated). This gives an indication of the dynamic heat dissipation capability of a device.

By comparing the temperature profiles inside the empty enclosure (Fig. 3) and on the thermal mass (Fig.4), it can be observed that the change of temperature inside the enclosure will be instantaneous, while the temperature change of the thermal mass has a certain delay. While the air temperature decreases to 10 ˚C, the temperature on the thermal mass is hotter, and this will contribute to the accumulation of condensed water or water vapour inside the enclosure at each cycles. The presence of the larger thermal mass (216 g) has led to an AH value of 57 $g \cdot m^{-3}$ at the last cycle, while only a level of 52 $g \cdot m^{-3}$ of AH has been measured in presence of thermal mass of 108 g (see Fig.4).

A heat sink is designed to maximize its surface area in contact with the cooling medium surrounding it, in this case air. The choice of material, its surface area, and the air velocity are the primary factors that affect the performance of a thermal mass. The most common heat sink materials are aluminium which has a thermal conductivity of 205 W/m·K (at 25 ˚C).

The bigger leak size of the casing (3 mm diameter) allowed better water vapour diffusion between internal and external environments, and also a better air flow due to temperature difference between inside and outside (natural convection). The higher air flow and the high thermal conductivity of the thermal mass combined with its large surface area resulted in the rapid transfer of thermal energy to the surrounding, cooler, air. This cooled the PCB at the same rate than the thermal mass which is in direct thermal contact with it.

The sudden increase of LC on the SIR PCB is a result of the increased moisture content of the vapour phase at higher temperature (50 ˚C), leading to more moisture adsorbed by the board [16].

The introduction of NaCl contamination on the surface of the PCBA has led to increase of LC as much as 3-4 orders of magnitude, representative of moisture condensation. The presence of the ionic residues will increase the water layer thickness (due to their hygroscopic nature) and increase the conductivity of the electrolyte. The optical pictures did not show any ECM, confirming that dendrites did not cause these intermittent drops. This is highly significant from the point of view of the application of electronic devices, as it indicates that the temperature differential that leads to a significant level of water layer formation on the surface can be reduced due to the presence of ionic contamination [17] [18] [5].

V. Conclusion

1. The time constant for temperature is shorter than the time constant for humidity equilibrium. Even at constant humidity, the outdoor cycling temperature will lead to a cycling humidity inside the electronic device. In the presence of openings, such as feedthrough of cables, or ventilation, the equilibrium will be reached faster.

2. The delay of temperature change between the external conditions and the thermal mass inside an electronic device will lead to a “pumping effect”, with accumulation of condensed water inside the enclosure at each cycle of decreasing temperature.

3. The climatic critical factors for electronic reliability are high temperature and temperature cycling. The changes of internal temperature and humidity can lead to water condensation and evaporation cycles which are dangerous for the electronic assemblies and can cause electrical failures.

4. The thickness of the water layer on the electronic surfaces will depend on the presence, and on the level of contaminations such as ionic or hygroscopic compounds.

VI. Acknowledgements

Current research has been conducted as part of the ICCI project funded by the Danish Council for Independent Research, Technology and Production (FTP) and IN-SPE project funded by the Innovation Fund Denmark. The authors would like to acknowledge the commitment and help of the industrial partners.

References

[1] S. Mottahed, B. D., Manoochehri, “Design considerations for electronic enclosures utilizing polymeric materials,” *Polym. - Plast. Technol. Eng.*, vol. 38, no. 5, pp. 883 – 925, 1999.

[2] A. H. J. Jacobsen, J. P. Krog, L. Rimestadt, A. Riis, “Using basic physics to solve climatic challenges for electronics,” *IEEE Ind. Electron. Mag.*, 2014.

[3] K. S. Hansen, M. S. Jellesen, P. Moller, P. J. S. Westermann, and R. Ambat, “Effect of solder flux residues on corrosion of electronics,” in *Annual Reliability and Maintainability Symposium*, 2009, pp. 502–508.

[4] V. Verdingovas, M. S. Jellesen, and R. Ambat, “Influence of sodium chloride and weak organic acids (flux residues) on electrochemical migration of tin on surface mount chip components,” *Corros. Eng. Sci. Technol.*, vol. 48, no. 6, pp. 426–435, 2013.

[5] V. Verdingovas, M. S. Jellesen, and R. Ambat, “Impact of NaCl Contamination and Climatic Conditions on the Reliability of Printed Circuit Board Assemblies,” *IEEE Trans. Device Mater. Reliab.*, vol. 14, no. 1, pp. 42–51, Mar. 2014.

[6] V. Verdingovas, M. S. Jellesen, and R. Ambat, “Solder Flux Residues and Humidity-Related Failures in Electronics: Relative Effects of Weak Organic Acids Used in No-Clean Flux Systems,” *J. Electron. Mater.*, vol. 44, no. 4, pp. 1116–1127, Jan. 2015.

[7] H. Conseil, M. Stendahl Jellesen, and R. Ambat, “Contamination profile on typical printed circuit board assemblies vs soldering process,” *Solder. Surf. Mt. Technol.*, vol. 26, no. 4, pp. 194–202, Aug. 2014.

[8] M. S. Jellesen, B. D. Mikkelsen, and R. Ambat, “Printed circuit board surface finish and effects of chloride contamination , electric field , and humidity on corrosion reliability,” in *Eurocorr 2013*, 2013.

[9] J. D. Sinclair, L. A. Psota-Kelty, G. A. Peins, “Key word index: Indoor air quality, ionic contamination, dust, aerosol deposition.,” *Atmos. Environ.*, vol. 26A, no. 5, pp. 871–882, 1992.

[10] P. R. Roberge, R. D. Klassen, and P. W. Haberecht, “Atmospheric corrosivity modeling - a review,” *Mater. Des.*, vol. 23, pp. 321–330, 2002.

[11] C. Schimpf, K. Feldmann, C. Matzner, and a. Steinke, “Failure of electronic devices due to condensation,” *Microsyst. Technol.*, vol. 15, no. 1, pp. 123–127, Jun. 2008.

[12] M. S. Jellesen, D. Minzari, U. Rathinavelu, P. Møller, and R. Ambat, “Investigation of Electronic Corrosion at Device Level,” *ECS Trans.*, vol. 25, no. 30, pp. 1–14, 2010.

[13] D. Minzari, M. S. Jellesen, P. Møller, P. Wahlberg, and R. Ambat, “Electrochemical Migration on Electronic Chip Resistors in Chloride Environments,” *IEEE Trans. Device Mater. Reliab.*, vol. 9, no. 3, pp. 392–402, 2009.

[14] D. Minzari, “No Title,” Technical University of Denmark, 2010.

[15] “IPC standard J-STD-001D ‘Requirements for soldered electrical and electronic assemblies’.”.

[16] S. Zhan, M. H. Azarian, and M. Pecht, “Reliability of Printed Circuit Boards Processed Using No-Clean Flux Technology in Temperature–Humidity–Bias Conditions,” *IEEE Trans. Device Mater. Reliab.*, vol. 8, no. 2, pp. 426–434, Jun. 2008.

[17] C. Cirolia., F., Finan., “The effects of airborne contaminants on electronic power supplies,” in *IEEE Applied Power Electronics Conference and Exposition - APEC*, 2001, vol. 1, pp. 238 – 242.

[18] M. Tencer, “Conductive aqueous layer formation at the gel-substrate interface in equilibrium with 100% RH environment,” *IEEE Trans. Components Packag. Technol.*, vol. 23, no. 4, pp. 693–699, 2000.